IX International Conference on Computational Methods in Marine Engineering
MARINE 2021
I.M. Viola and F. Brennan (Eds)

ANALYSIS OF A FLOATING WAVE ENERGY CONVERTER INTERACTING WITH WAVES USING THE OVERSET FRAMEWORK

GABRIEL BARAJAS[*], JAVIER L. LARA[*], BENEDETTO DI PAOLO[*] AND IÑIGO J. LOSADA[*]

[*] IHCantabria, Instituto de Hidráulica Ambiental de La Universidad de Cantabria.
C/Isabel Torres No 15, Parque Científico y Tecnológico de Cantabria, 39011,
Santander, Spain

Key words: CFD, WEC, OpenFOAM, Overset mesh method, water waves.

Abstract. The aim of this work is to validate and analyze with the numerical model OpenFOAM, the nonlinear interaction of a WEC under regular waves using the Overset framework. Previous techniques, such as deforming grid approaches, present problems to handle large body motions when modelling wave-structure interactions. Therefore, by means of the Overset mesh technique, the interaction of a moored floating wave energy converter in free and moored decay tests and under regular waves are analyzed. Numerical results are compared with experimental data for validation and discussed. MooDy Library is used to compute the mooring restraints.

1 INTRODUCTION

Characterization of the interaction of waves and currents with wave energy converters (WEC) is one of the most challenging issues due to the relevance of the nonlinear physical processes involved. For example, in the structural design of this type of structures, forces acting on the bodies and mooring line tensions are needed, together with a dynamic analysis for evaluating the body response (surge, heave, sway, pitch, roll and yaw). Due to the complexity of the problem the main methodology exploited so far has been the physical modelling. In recent years, there has been a growing development of numerical models with the main goal of reducing the number of physical model tests to be carried out, as they are economically more expensive.

One of the main challenges regarding wave-floating structure interaction in CFD modelling is how handling the mesh motion to correctly reproduce the physical processes involved. Although several approaches are available in literature regarding mesh motion numerical implementations (Jasak and Tukovic 2010 [1], (also implemented in OpenFOAM environment), in Liu et al. 2017 [2]), the Overset mesh grid (Meakin Robert L., 1999 [3], Petersson N. Anders, 1999 [4], Suhs and Rogers, 2002 [5], Di Paolo, 2019 [6], Windt, 2018 [7], Pinguet, 2021 [8]) appears as the most precise and stable for large body displacements.

The aim of this work is to present the Overset mesh technique in OpenFOAM as an accurate tool for simulating moored floating wave energy converters under regular waves. The present work is organized in 3 sections as follows: first, the numerical model is presented; secondly, the experiments used for validation are described as well as the

numerical configuration, and several cases are analyzed in detail. Finally, some conclusions obtained from this work are stated.

2 NUMERICAL MODEL

Numerical simulations have been performed using IHFOAM (Higuera, 2013 [9], Di Paolo, 2021 [10, 11], a suite of tools built on the open-source platform OpenFOAM (ESI, 2021 [12], Jasak, 1996 [13]) which includes boundary conditions (waves, currents and waves&currents) and porous media solvers (Higuera, 2013 [9]) for coastal and offshore engineering applications. It can solve both three dimensional Reynolds Averaged Navier Stokes equations (RANS) and Volume Averaged Reynolds averaged Navier Stokes equations (VARANS) (Higuera, 2013 [9]) for two phase flows. In the present work, RANS equations have been solved, coupled to the Volume of Fluid (VOF) equation, the Overset mesh technique and the external library called MooDy [14].

2.1- Governing Equations

The RANS equations are represented by the mass (1) and momentum (2) conservation equations, coupled to the VOF (3) equation as follows:

$$\frac{\partial u_i}{\partial x_i} = 0 \tag{1}$$

$$\frac{\partial \rho u_i}{\partial t} + u_j \frac{\partial \rho u_i}{\partial x_j} = -g_j x_j \frac{\partial \rho}{\partial x_i} - \frac{\partial p^*}{\partial x_i} - \frac{\partial}{\partial x_j} \mu_{eff} \left(\frac{\partial \rho u_i}{\partial x_j} + \frac{\partial \rho u_j}{\partial x_i} \right) \tag{2}$$

$$\frac{\partial \alpha}{\partial t} + \frac{\partial u_i \alpha}{\partial x_i} + \frac{\partial u_{ci}\, \alpha(1-\alpha)}{\partial x_i} = 0 \tag{3}$$

where u_i is the velocity (m/s), x_i the Cartesian coordinates (m), g_j the components of the gravitational acceleration (m/s2), ρ the density of the fluid (kg/m3), p^* the ensemble averaged pressure in excess of hydrostatic, defined as $p^* = p - \rho\, g_j\, x_j$ (Pa), being p the total pressure, α the volume fraction indicator function (-) , which is assumed to be 1 for the water phase and 0 for the air. μ_{eff} is the effective dynamic viscosity (Pa · s) that is defined as $\mu_{eff} = \mu + \rho\, \nu_t$ and takes into account the dynamic molecular (μ) and the turbulent viscosity effects ($\rho\, \nu_t$); ν_t is the eddy viscosity (m2/s), which is provided by the turbulence closure (k-omega-SST model from Larsen and Fuhrman, 2018 [15]). u_{ci} is the compression velocity.

2.2- Overset Mesh technique

The Overset mesh technique is described in Romano, 2020 [16]. It is based on the use of two domains: a moving domain to describe the displacements of the floating body and a background domain to characterize the numerical wave tank. The overlapping of both creates a new mesh that can represent complex geometries and large displacements while maintaining a good quality mesh.

2.3- Mooring Solver: MooDy

The external library called MooDy [14] is used for computing the mooring cable dynamics, implemented as a hp-adaptive cable solver based on the discontinuous Galerkin method. The numerical implementation and validation of MooDy is described in [14].

3 VALIDATION AGAINST NUMERICAL DATA

The main objective of this work is to present a comprehensive analysis of the use of the Overset mesh technique to replicate the motion of a moored floating WEC. Several validations are shown: free decay tests of a free buoy, free decay tests of a moored buoy and regular waves interaction with a moored buoy.

3.1 - Numerical Setup

A numerical wave tank has been developed to replicate the experimental and numerical analysis from Palm, 2016 [17]. The basin is 8m long, 8m wide and 2m high. The numerical domain has been defined wider than the numerical wave flume described by Palm [17], in order to avoid the reflections that occur when the generated waves reach the side walls.

The floating body is of the same dimensions as described in Palm, 2016 [17] and Moura, 2016 [18]. It is a truncated cylinder of diameter D=0.515m, mass M=35.85kg and moment of inertia around the center of gravity Ixx=0.9 kg m2. It is anchored to the bottom with three mooring cables, placed symmetrically 120º apart, with one cable attached on the leeward side directed along the propagation direction of the waves (Fig.1, left panel). An initial water depth of h=0.9m is defined. The mooring system is modelled by means of the Moody library [14] and the numerical parameters are compiled from measurable quantities given in [18]. The k-omega-SST model from Larsen and Fuhrman, 2018 [15] has been used for turbulence modelling as it provides a stable solution for the over production of turbulence levels beneath waves.

Shallow water wave absorption is defined as the boundary condition at the four side walls (left, right, front and back, in Fig. 1). A non-slip boundary condition is defined to the flat bottom, the top is defined as an open boundary.

For all the simulations presented in this work, the floating object motion is defined by six degrees of freedom (heave, sway, surge, pitch, roll and yaw). MULES is used to solve the VOF equation and the PIMPLE algorithm to solve the velocity-pressure coupling in the fundamental equations. In order to prove the robustness of the Overset mesh method with the MooDy library, the resulting acceleration from the Six degrees of freedom (6DoF) solver in OpenFOAM is not damped or reduced by any means.

A preliminary grid refinement study is carried out, following the approach described in Devolder, 2017 [19]. Thus, the background domain is characterized by a cell resolution of 0.0625m along the x and y directions, and 0.0312m along the z direction. The moving domain is characterized by a cell resolution of 0.0312m in all three directions. The computational domain is discretized into a structured grid (Fig. 1, right panel) and contains 4.3M cells.

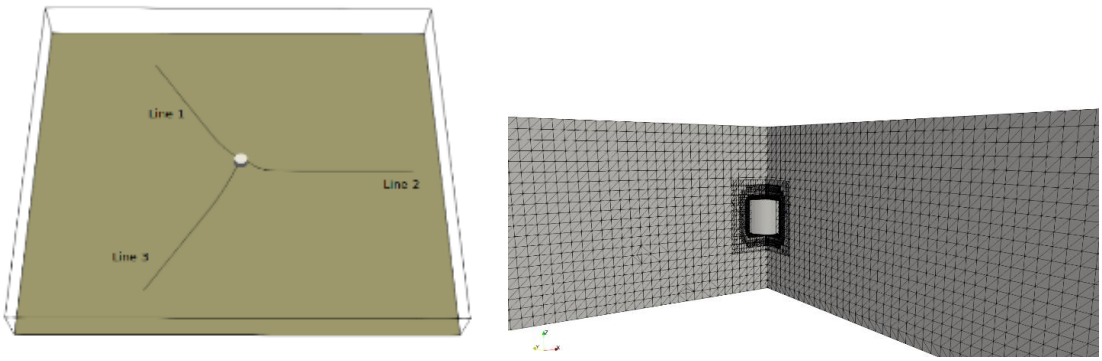

Figure 1, Left panel, perspective view of the numerical domain with the buoy and the three chains placed in the initial position. Right panel, snapshot of the final mesh, including the moving domain and the background mesh.

3.2 - Free decay test of a WEC

In this section, the motion of a free buoy is presented when released from a given excitation in heave (initial offset δ=0.075m) and pitch (initial offset δ=9.898º). Time series of comparison between the present work (Overset mesh method) and the numerical (deforming grid) and experimental work carried out by Palm, 2016 [17] are shown in Fig. 2.

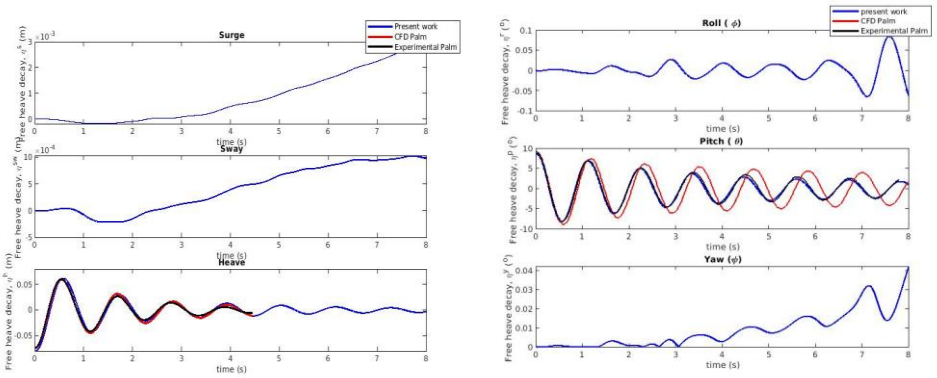

Figure 2: Left panel, free decay of the buoy when released from a given excitation in heave (surge, sway and heave), right panel, free decay of the buoy when released from a given excitation in pitch (roll, pitch and yaw). Present work (blue line), numerical (black line) and experimental (red line) by Palm [17].

Fig. 2 shows the comparison between present work (blue line) and the numerical work (black line) and the experimental (red line) by Palm, 2016 [17] when the buoy is released from a given excitation. As it is a free buoy, no mooring restraints are attached.

The responses from both CFD techniques (deforming mesh and Overset mesh technique) are in good agreement. The damping of the oscillation obtained from the Overset mesh technique is similar to the results from the mesh morphing method and the numerical experiments.

3.3 - Free decay test of a moored WEC

In this section, the motion of a moored buoy is presented when it is released from a given excitation in surge (initial offset δ=0.114m, case-A), heave (initial offset δ=0.076m, case-B) and pitch (initial offset δ=11.353º, case-C). Time series of comparison between the present work (Overset mesh method) and the numerical (deforming grid) and experimental work carried out by Palm, 2016 [17] are displayed in Fig. 3, 4 and 5, respectively.

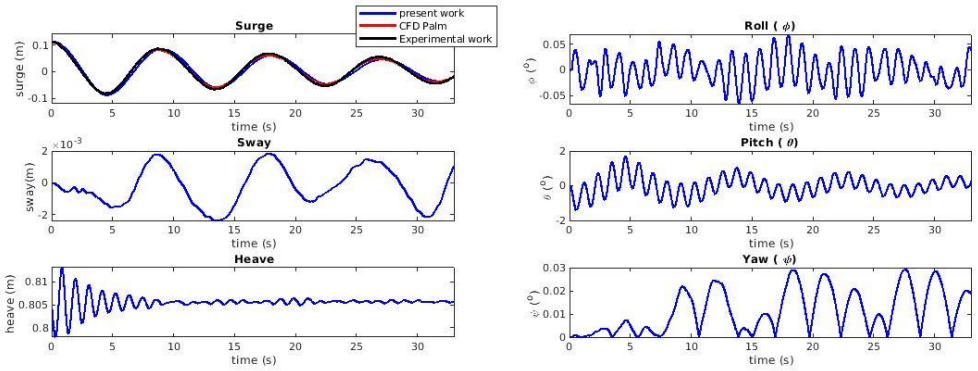

Figure 3: Six degrees of motion for a free decay of the moored buoy when released from a given excitation in surge (δ= 0,114m). Present work (blue line), numerical (black line) and experimental (red line) by Palm [17].

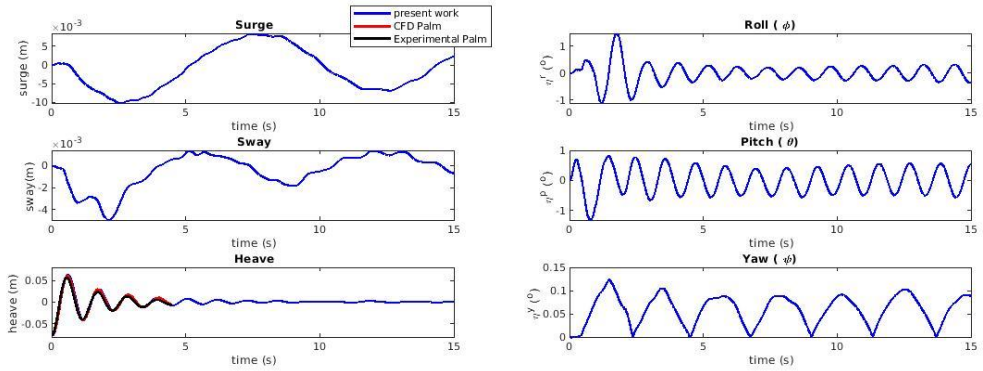

Figure 4: Six degrees of motion for a free decay of the moored buoy when released from a given excitation in heave (δ= 0,076m). Present work (blue line), numerical (black line) and experimental (red line) by Palm [17].

In Figs. 3, 4 and 5, it is observable a good agreement between the present work and the experimental and previous numerical results. Moreover, the period of oscillation for both numerical techniques (deforming mesh and Overset mesh technique) are the same for the three cases.

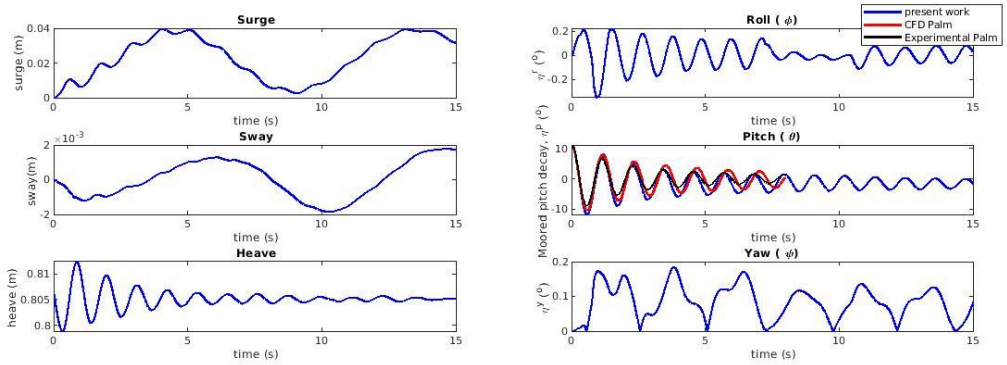

Figure 5: Six degrees of motion for a free decay of the moored buoy when released from a given excitation in pitch (δ= 13.353°). Present work (blue line), numerical (black line) and experimental (red line) by Palm [17].

The surge and heave response are equally damped than the experimental results for both numerical approaches (Fig. 3 and 4). It can be seen a difference in the damping of the oscillations for the pitch decay case (Fig. 5) between both numerical approaches and the experiments. Moreover, the results from the present work are in phase with the experimental data.

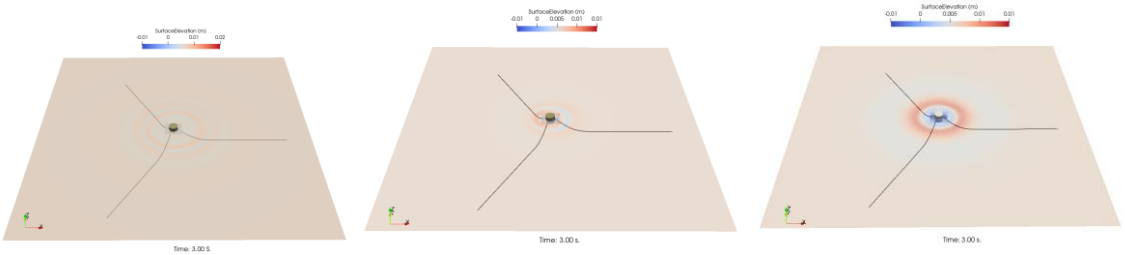

Figure 6: Left panel, surface elevation (perspective view, free surface VOF=0.5), case-A (left), case-B (middle) and case-C (right).

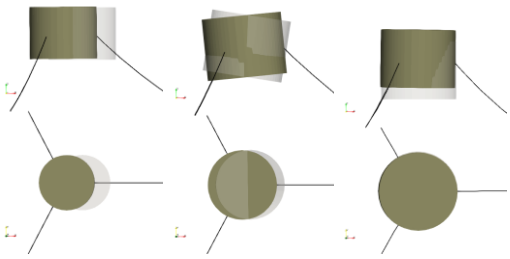

Figure 7: Top panel: displacement of the buoy from its initial position (side view, plane XZ), case-A (left), case-B (middle) and case-C (right). Bottom panel, displacement of the buoy from its initial position (top view plane XY), case-A (left), case-B (middle) and case-C (right)

Fig. 6 shows the surface elevation over the free surface (left panel) and Fig. 7 shows the displacement of the buoy from its initial position on a side view (top panels) and the

displacement of the buoy from its initial position on a top view plane (bottom panels) for the three decay tests, respectively. It is seen that the lateral wall does not have a significant influence on the flux around body

3.4 - Regular waves interaction with a moored WEC.

In this section, numerical simulations of the moored buoy interacting with regular waves are compared. Two sets of experiments are carried out with different wave heights (H=0.04m and H=0.08m), each of them with three different periods (T=1.0s, T=1.2s and T=1.4s).

The dimensions of the numerical wave tank are reduced in this case in order to minimize the computational costs. The basin is now 6m long, 5m wide and 2m high. As it can be observed the numerical domain is defined the same as the one used in Palm et al. 2016 [17], without including the relaxation zones. Thus, the buoy was surrounded by 3m. of free computational domain on both sides of its initial position.

Wave generation and active absorption are defined as boundary conditions at the inlet (in Fig. 1, left panel, left boundary condition), while only shallow water active absorption has been used at the outlet (in Fig. 1, left panel, right boundary condition) of the domain. Velocity and free surface level are set at the inlet boundary for generating and absorbing waves at the same time. Stokes 5th order waves are generated. A non-slip boundary condition is defined to the flat bottom, the top is defined as an open boundary, and a slip condition has been applied at the side walls.

The background domain and the moving domain are characterized by a cell resolution of 0.024m along the x and y directions, and 0.008m along the z direction. The computational domain is discretized into a structured grid and it contains 13.4M cells.

Time series of comparison between the present work and the numerical and experimental work carried out by Palm, 2016 [17] for 3 wave periods are analyzed. Fig. 7 and 8 shows the wave elevation of the incoming waves, and the response in surge, heave and pitch of the moored floating buoy for the 6 cases.

Again, it can be seen an overall good agreement between the present work and the experimental and previous numerical results, except for the surge motion. These anomalous results were noticed by Palm, 2016 [17] and are analyzed more in detail in Fig. 9.

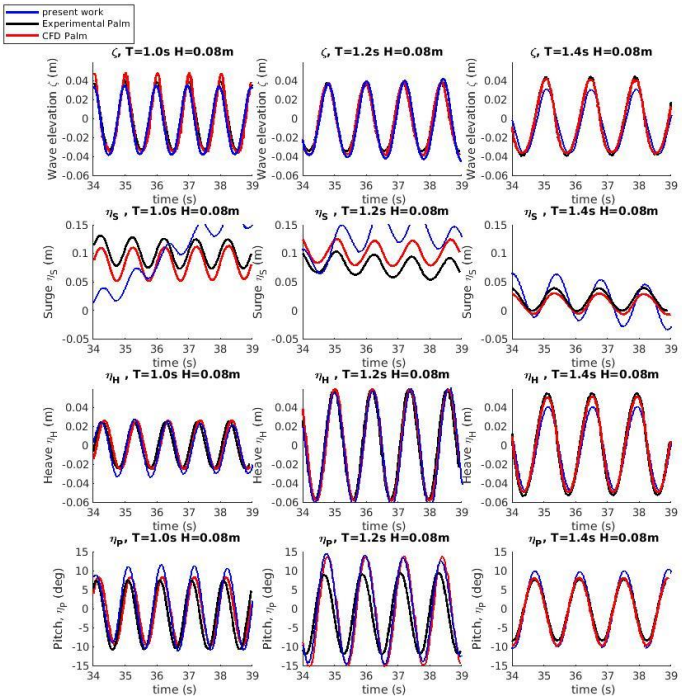

Figure 7: Regular waves with target wave height H=0.04m (T=1.0s, T=1.2s and T=1.4s). Present work (blue line), numerical (black line) and experimental (red line) by Palm [17].

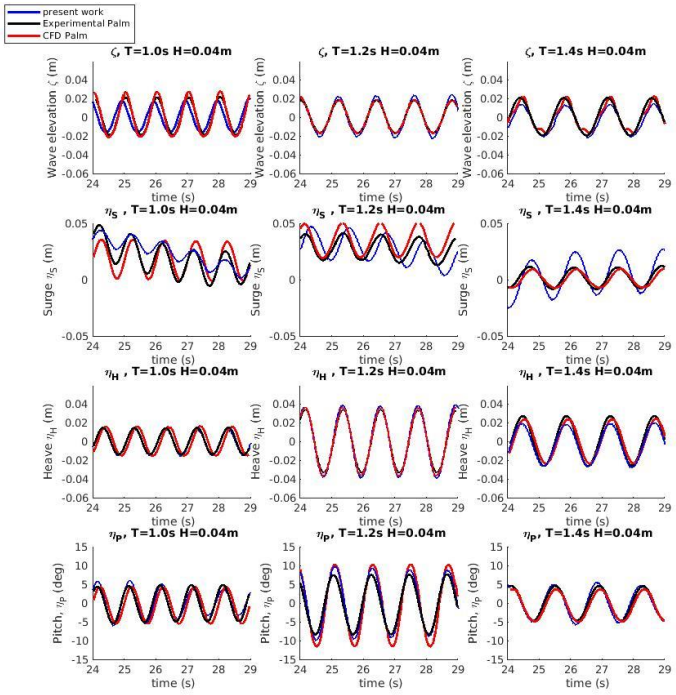

Figure 8: Regular waves with target wave height H=0.08m (T=1.0s, T=1.2s and T=1.4s). Present work (blue line), numerical (black line) and experimental (red line) by Palm [17].

As it is clearly seen from Fig. 9, wave elevation, heave and pitch fit very well with experimental data, but surge results are influenced by a numerical oscillation that will be damped over time. From the authors point of view, it is believed that it might be caused by a very big acceleration induced by the firsts waves when interacting with the still buoy; choosing a bigger ramping time would attenuate this effect.

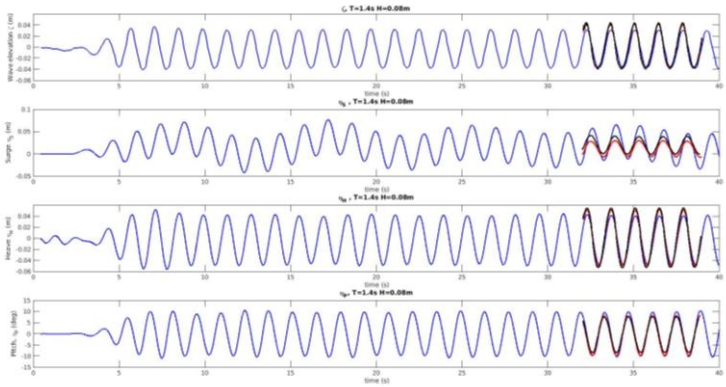

Figure 9: Wave elevation, surge, heave and pitch for H=0.08m, T=1.4s. Present work (blue line), numerical (black line) and experimental (red line) by Palm [3].

Finally, Fig. 10 and 11 shows a top view of the surface elevation (in meters) on the free surface (VOF=0.5) generated by the incoming waves. Results for cases with H=0.04m are presented in Fig. 10 (first, second and third, for T=1.0s, T=1.2s and T=1.4 s respectively) and for cases with H=0.08m in Fig.11 (first, second and third,, for T=1.0s, T=1.2s and T=1.4 s respectively).It can be seen that when increasing the wave period, the wave patterns are less induced by the interaction with the floating body, as there is longer distance between the peaks of two consecutive waves. Again, it can be seen that side walls do not have a significant influence on the flux around the body.

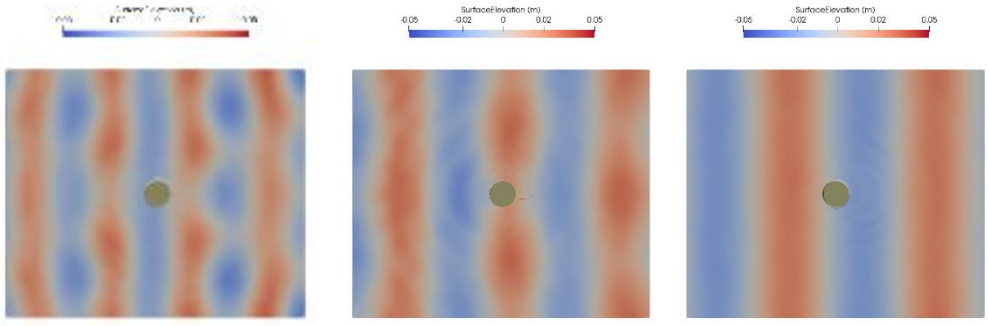

Figure 10: Surface elevation(m) plotted on the free surface (VOF=0.5). Top panel (for H=0.04m, T=1.0s, T=1.2s and T=1.4s) and bottom panel (for H=0.08m, T=1.0s, T=1.2s and T=1.4s)

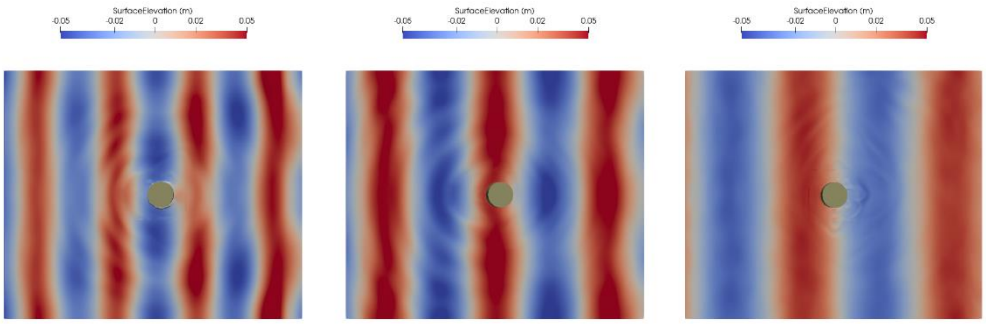

Figure 11: Surface elevation(m) plotted on the free surface (VOF=0.5). Top panel (for H=0.04m, T=1.0s, T=1.2s and T=1.4s) and bottom panel (for H=0.08m, T=1.0s, T=1.2s and T=1.4s)

4 CONCLUSIONS

In this work, the interaction of a moored floating wave energy converter in a free and moored decay tests and under regular waves are analyzed by means of the open-source numerical model OpenFOAM [12]. The Overset framework is used for modeling the displacement of a WEC [17], Moody library [14] is used to compute the mooring restraints, and the IHFOAM [9] suite to generate the boundary conditions.

By analyzing the decay tests and regular wave cases, it is remarkable a good agreement between the present work and the experimental data [17]. Moreover, the comparison between two different numerical techniques for simulating moving bodies, deforming grid [17] and Overset mesh method (present work) show an overall good agreement between them and against the experimental data.

As it is known, deforming grid approaches cannot handle large body displacements. Therefore, as a conclusion, the Overset mesh technique may be used for analyzing more complex geometry and extreme hydrodynamic conditions. Further work will be done to improve the accuracy of the Overset mesh method in predicting wave fields and body response.

REFERENCES

[1] H. Jasak, Ž. Tukovic, Dynamic mesh handling in openfoam applied to fluid-structure interaction simulations, in: Proceedings of the V European Conference on Computational Fluid Dynamics ECCOMAS (2010).

[2] Y. Liu, Q. Xiao, A. Incecik, C. Peyrard, D. Wan. Establishing a fully coupled cfd analysis tool for floating offshore wind turbines, Renewable Energy 112 (2017) 280–301.

[3] R. Meakin, Composite overset structured grids, chap. 11 (1999).

[4] N. A. Petersson, Hole-cutting for three-dimensional overlapping grids, SIAM Journal on Scientific Computing 21 (2) (1999) 646–665

[5] N. Suhs, S. Rogers, W. Dietz, Pegasus 5: An automated pre-processor for overset-grid cfd, in: 32nd AIAA Fluid Dynamics Conference and Exhibit, (2002), p. 3186.

[6] Di Paolo, B., Lara, J.L., Barajas, G., Paci, A. and Losada, I.J., (2019), June. Numerical analysis of wave and current interaction with moored floating bodies using overset method. In ASME 2018 37th International Conference on Ocean, Offshore and Arctic Engineering (pp. V002T08A037- V002T08A037). American Society of Mechanical Engineers.

[7] Windt, C., Davidson, J., Akram, B., Ringwood, J.V., (2018). Performance Assessment of the Overset Grid Method for Numerical Wave Tank Experiments in the OpenFOAM Environment, ASME 2018 37th International Conference on Ocean, Offshore and Arctic Engineering DOI: 10.1115/OMAE2018-77564

[8] Pinguet, R., Kanner, S., Benoit, M., Molin, B. (2021). Modeling the dynamics of freely-floating offshore wind turbine subject to waves with an open-source overset mesh method. 3th International offshore Wind Technical Conference. IOWT2021-3536.

[9] P. Higuera, J. L. Lara, I. J. Losada, Realistic wave generation and active wave absorption for Navier-Stokes models: Application to OpenFOAM, Coastal Engineering 71 (2013) 102–118.

[10] Di Paolo, B.; Lara, J.L.; Barajas, G.; Losada, Í.J. Wave and structure interaction using multi-domain couplings for Navier-Stokes solvers in OpenFOAM®. Part I: Implementation and validation. Coast. Eng. 2020, 103799. (2021)

[11] Di Paolo, B.; Lara, J.L.; Barajas, G.; Losada, Í.J. Waves and structure interaction using multi-domain couplings for Navier-Stokes solvers in OpenFOAM®. Part II: Validation and application to complex cases. Coastal Engineering 164, 103818. (2021).

[12] ESI-Group, Openfoam the open source cfd toolbox. URL https://www.openfoam.com/

[13] Jasak, H., Error analysis and estimation for finite volume method with applications to fluid flow. PhD Thesis. (1996).

[14] J. Palm, C. Eskilsson, L. Bergdahl. An hp-adaptive discontinuous Galerkin method for modelling snap loads in mooring cables. Ocean Engineering, 144:266-276, (2017).

[15] B. E. Larsen, D. R. Fuhrman, On the over-production of turbulence beneath surface waves in Reynolds-Averaged Navier-Stokes models, Journal of Fluid Mechanics 853 (2018) 419– 460

[16] A Romano, JL Lara, G Barajas, Benedetto Di Paolo, G Bellotti, M Di Risio, IJ Losada, P De Girolamo Tsunamis Generated by Submerged Landslides: Numerical Analysis of the Near-Field Wave Characteristics Journal of Geophysical Research: Oceans 125 (7), e2020JC016157, (2020).

[17] J. Palm, C. Eskilsson, G. M. Paredes, L. Bergdahl. Coupled mooring analysis for floating wave energy converters using CFD: Formulation and validation. International Journal of Marine Energy, ISSN: 2214-1669, Vol: 16, Page: 83

[18] Moura Paredes, G., Palm, J., Eskilsson, C., Bergdahl, L., Taveira Pinto, F., (2016). Experimental investigation of mooring configurations for wave energy converters. Int. J. Mar. Energy 15, 56–67. https://doi.org/10.1016/j.ijome.2016.04.009

[19] B. Devolder, P. Rauwoens, P. Troch, Application of a buoyancy-modified k-ω sst turbulence model to simulate wave run-up around a monopile subjected to regular waves using openfoam, Coastal Engineering 125 (2017) 81–94.